Published in final edited form as:
J Magn Reson. 2009 April ; 197(2): 145–152. doi:10.1016/j.jmr.2008.12.011.

Dipolar recoupling in solid state NMR by phase alternating pulse sequences

J. Lin[*], **M. Bayro**[†], **R. G. Griffin**[‡], and **N. Khaneja**[§]

[*] School of Engineering and Applied Sciences, Harvard University, Cambridge, MA 02138

[†] Department of Chemistry and Francis Bitter Lab, MIT

[‡] Department of Chemistry and Francis Bitter Lab, MIT

Abstract

We describe some new developments in the methodology of making heteronuclear and homonuclear recoupling experiments in solid state NMR insensitive to rf-inhomogeneity by phase alternating the irradiation on the spin system every rotor period. By incorporating delays of half rotor periods in the pulse sequences, these phase alternating experiments can be made γ encoded. The proposed methodology is conceptually different from the standard methods of making recoupling experiments robust by the use of ramps and adiabatic pulses in the recoupling periods. We show how the concept of phase alternation can be incorporated in the design of homonuclear recoupling experiments that are both insensitive to chemical-shift dispersion and rf-inhomogeneity.

1 Introduction

An important application of solid state nuclear magnetic resonance (NMR) spectroscopy is in structural analysis of “insoluble” protein structures such as membrane proteins, fibrils, and extracellular matrix proteins which are exceedingly difficult to analyze using conventional atomic-resolution structure determination methods, including liquid-state NMR and X-ray crystallography [1,2,3,4,5]. The goal of studying increasingly complex molecular systems is a strong motivation for the development of improved solid-state NMR methods. The paper describes a set of new principles for design of heteronuclear and homonuclear dipolar recoupling experiments that are both broadband and insensitive of rf-field inhomogeneities. The merits of the proposed techniques with respect to state of the art methods is discussed.

For solids, the internal Hamiltonian not only contains isotropic interactions, such as isotropic chemical shifts and scalar *J* couplings, but also anisotropic (i.e., orientation dependent) chemical shifts and dipole-dipole coupling interactions in the case of coupled spin-1/2 nuclei. This implies that each molecule/crystallite in a “powder” sample may exhibit different nuclear spin interactions leading to severe line broadening and thereby reduced spectral resolution and sensitivity. This problem may be alleviated using magic-angle spinning (MAS), which averages these interactions and hereby results in high-resolution conditions for solid samples. However, this also results in loss of useful parts of the anisotropic interactions like dipolar

§To whom correspondence may be addressed. School of Engineering and Applied Sciences, Harvard University, Cambridge, MA 02138. Email: navin@hrl.harvard.edu.

couplings, which carry information about distances between nuclei and can help in obtaining structural information. This has triggered the development of dipolar recoupling techniques [6,11,12,13,14,15,16], which selectively reintroduce these couplings to enable measurement of internuclear distances, torsion angles, and transfer of magnetization from spin to spin in the molecule. Such recoupling experiments are the building blocks of essentially all biological solid-state NMR experiments using “powder” samples. However, the recoupling experiments are sensitive to the amplitude of the radio-frequency fields and the orientation dependence of the dipolar coupling interaction.

The latter challenge motivates the present paper, where we present methods for making dipolar recoupling experiments insensitive to rf-inhomogeneity and Hartmann-Hahn mismatch by phase alternating the irradiation on the spins every rotor period. In [7], it was shown that this simple technique makes recoupling experiments less sensitive to the dispersion in the strength of the radio-frequency field. These experiments however do not achieve uniform transfer efficiency for all γ, where γ represents the rotation of the crystallite around the rotor axis. By introducing, half rotor period delays in the middle of the proposed phase-alternating recoupling blocks, the recoupling is made insensitive to the angle γ. One standard technique for making recoupling experiments robust to Hartmann Hahn mismatch is by using ramps or shaped adiabatic pulses on the rf-power during the recoupling period. The described methodology is conceptually very different. The main contribution of this paper is the development of broadband homonuclear recoupling experiments that are robust to rf-inhomogeneity by using this concept of phase alternation. The main ideas described here are further developments of the recent work [38] on broadband homonuclear recoupling. We show that by using phase alternation, we can make experiments in [38], less sensitive to rf-inhomogeneity.

Phase alternating pulse sequences have appeared in solid state NMR experiments in numerous context before [7,8,9,10]. The main contribution of this paper is further development of this methodology as a means to design robust recoupling experiments in various contexts.

2 Theory

Consider two coupled heteronuclear spins I and S under magic angle spinning. The spins are irradiated with x phase rf fields at their Larmor frequencies. In a double-rotating Zeeman frame, rotating with both the spins at their Larmor frequency, the Hamiltonian of the spin system takes the form

$$H(t)=\omega_I(t)I_z+\omega_S(t)S_z+\omega_{IS}(t)2I_zS_z+\omega^I_{rf}(t)I_x+\omega^S_{rf}(t)S_x, \quad (1)$$

where $\omega_I(t)$, $\omega_S(t)$, and $\omega_{IS}(t)$ represent time-varying chemical shifts for the two spins I and S and the coupling between them, respectively. These interactions may be expressed as a Fourier series

$$\omega_\lambda(t)=\sum_{m=-2}^{2}\omega^m_\lambda\exp(im\omega_r t), \quad (2)$$

where ω_r is the spinning frequency (in angular units) and $\tau_r=\frac{2\pi}{\omega_r}$ is the rotor period. The coefficients $\omega_\lambda(\lambda = I, S, IS)$ reflect the dependence on the physical parameters like the isotropic chemical shift, anisotropic chemical shift, the dipole-dipole coupling constant and through this the internuclear distance [24]. $\omega^I_{rf}(t)$ and $\omega^S_{rf}(t)$ are the amplitudes of the rf fields on spins I

and *S*, respectively. If the rf-field strengths on the two spins is chosen to be integral (or half integral) multiples of the spinning frequency, i.e., $\omega_{rf}^{I}=p\omega_r$ and $\omega_{rf}^{S}=q\omega_r$, then the Hamiltonian for the dipole-dipole coupling in the interaction frame of the rf-irradiation averages over a rotor period to

$$\begin{aligned}\overline{H}=&\tfrac{1}{4}\{(\omega_{IS}^{-(p+q)}+\omega_{IS}^{(p+q)})(2I_zS_z-2I_yS_y)\\&+(\omega_{IS}^{-(p-q)}+\omega_{IS}^{(p-q)})(2I_zS_z+2I_yS_y)\\&-i(\omega_{IS}^{-(p+q)}-\omega_{IS}^{(p+q)})(2I_zS_y+2I_yS_z)\\&i(\omega_{IS}^{-(p-q)}-\omega_{IS}^{(p-q)})(2I_zS_y-2I_yS_z)\}\end{aligned} \tag{3}$$

Choosing $p-q=-1$ and $|p+q|>2$, we prepare the effective Hamiltonian,

$$H_{dcp}(\gamma)=\kappa\{\cos(\gamma)(I_zS_z+I_yS_y)-\sin(\gamma)(I_zS_y-I_yS_z)\}, \tag{4}$$

where λ as before is the Euler angle discriminating the crystallites by rotation around the rotor axis. This is the standard DCP experiment [6]. The scaling factor

$$\kappa=\frac{1}{2\sqrt{2}}b_{IS}\sin(2\beta), \tag{5}$$

depends on the dipole-dipole coupling constant b_{IS} and the angle β between the internuclear axis and the rotor axis.

2.1 MOIST experiment

The effective Hamiltonian H_{dcp} mediates the coherence transfer $I_x \rightarrow S_x$ with an efficiency independent of the γ Euler angle. This transfer experiment is however sensitive to rf-inhomogeneity as described below. We consider rf-inhomogeneity on the two channels, such that rf-amplitude on the *I* channel is $\omega_{rf}^{I}=p(1+\varepsilon_I)\omega_r$ and rf-amplitude on the *S* channel is $\omega_{rf}^{S}=q(1+\varepsilon_S)\omega_r$. Here ε_I and ε_S represent the rf-inhomogeneity on the two channels *I* and *S* respectively.

In the interaction frame of the rf-irradiation, with nominal rf-strength $p\omega_r$ and $q\omega_r$, the natural Hamiltonian of the spin system averages to

$$\tilde{H}(\gamma)=H_{dcp}(\gamma)+\varepsilon^{-}\omega_r\frac{I_x-S_x}{2}+\varepsilon^{+}\omega_r\frac{I_x+S_x}{2}, \tag{6}$$

where $\varepsilon^{-}=\frac{\varepsilon_I-\varepsilon_S}{2}$ and $\varepsilon^{+}=\frac{\varepsilon_I+\varepsilon_S}{2}$. Let operators X^{-}, Y^{-} and Z^{-} represent the zero quantum operators $\frac{I_x-S_x}{2}$, $I_z S_z + I_y S_y$ and $I_z S_y - I_y S_z$ respectively. Similarly, X^{+} Y^{+} and Z^{+} represent the double quantum operators $\frac{I_x+S_x}{2}$, $I_z S_z - I_y S_y$ and $I_z S_y + I_y S_z$ respectively. The DCP Hamiltonian in Eq. (4) inverts the operator X^{-} in the zero quantum frame as depicted by the trajectory *A* in Fig. 1. In the presence of the Hartman Hahn mismatch, measured by the parameter ε^{-}, the operator X^{-} executes a rotation around the tilted axis leading to poor inversion, as depicted by trajectory *B* in Fig. 1.

Fig. 2A shows the efficiency η of $^{15}N \rightarrow {}^{13}C$, coherence transfer for the DCP experiment as a function of the mixing time τ_d. The build up curve is shown for different (increasing) values of ε^-. Observe that even for a small mismatch, corresponding to ε^-=.01, (1% of the rotor frequency), the efficiency of coherence transfer is significantly reduced. This sensitivity to mismatch can be significantly reduced by introducing the concept of phase-alternating pulse sequences.

We now describe the concept of phase-alternating pulse sequences as introduced in [7] for compensating rf-inhomogeneity in the system. Consider the pulse sequence in Fig. 3A, where the phase on both *I* and *S* channel is changed between $+x$ and $-x$ every rotor period. In [7], this experiment is called MOIST. To analyze the effect of this pulse sequence, in Eq. 6, we can omit the operator X^+, as it commutes with all operators in the zero quantum frame. In the interaction frame of the rf-field, the effective Hamiltonian in the first rotor period is

$$H_1 = H_{dcp}(\gamma) + \varepsilon^- \omega_r X^-, \tag{7}$$

and the effective Hamiltonian in the second rotor period is

$$H_2 = H_{dcp}(-\gamma) - \varepsilon^- \omega_r X^-, \tag{8}$$

The effective Hamiltonian from the phase alternation is

$$\frac{H_1 + H_2}{2} \sim \frac{\kappa}{2}\cos(\gamma)(I_z S_z + I_y S_y),$$

where we have used the small flip angle approximation ($\kappa\, \tau_r \ll 1$) and assumed that

$$\exp(-iH_1\tau_1)\exp(-iH_2\tau_r) \sim \exp(-i(H_1+H_2)\tau_r).$$

This Hamiltonian is not γ encoded. The resulting efficiency of transfer is lower as compared to the γ encoded experiments. Fig. 2B shows the transfer efficiency as a function of the mixing time for the phase alternating pulse sequence for different degrees of rf-inhomogeneity. Comparison to Fig. 2A shows that this sequence is more robust to rf-inhomogeneity.

2.2 PATCHED experiment

We now present a method to make this phase alternating pulse sequence γ encoded. We call this experiment PATCHED (**P**hase **A**lterna**t**ing experiment **C**ompensated by **H**alf rotor p**E**riod **D**elays). Fig. 3B shows the pulse sequence, consisting of a five rotor period building block, which is subsequently repeated many times, depending on the desired mixing period.

In the interaction frame of the nominal rf-irradiation, the first and third rotor period prepares the same effective Hamiltonian H_1 as in Eq. (7). The second rotor period prepares the same effective Hamiltonian H_2 as in Eq. (8). Following the third rotor period, a half rotor period delay moves the crystallites with angle γ to $\gamma + \pi$. In the final recoupling period, one prepares the effective Hamiltonian,

$$H_4=H_{dcp}(-(\gamma+\pi)) - \varepsilon^{-}\omega_r X^{-}. \quad (9)$$

Again, using the small angle approximation, we sum up the four Hamiltonians to get the effective Hamiltonian $\bar{H}$, such that

$$4\bar{H}=(H_{dcp}(\gamma)+\varepsilon^{-}\omega_r X^{-})+(H_{dcp}(-\gamma) - \varepsilon^{-}\omega_r X^{-})+ (H_{dcp}(\gamma)+\varepsilon^{-}\omega_r X^{-})+(H_{dcp}(-\gamma - \pi)+\varepsilon^{-}\omega_r X^{-}).$$

The resulting effective Hamiltonian $\bar{H}$ to leading order is then

$$\bar{H}=\frac{2\kappa}{5}\{\cos(\gamma)(I_z S_z+I_y S_y) - \sin(\gamma)(I_z S_y - I_y S_z)\}.$$

This is a γ encoded Hamiltonian, simply scaled down by a factor of $\frac{2}{5}$. To leading order, the effect of inhomogeneous rf-field gets canceled. Fig. 2B and Fig. 2C shows the transfer efficiency as a function of the mixing time for the presented phase-alternating and gamma-encoded phase alternating pulse sequence for different rf-inhomogeneity. The sequence achieves the same transfer efficiency as the γ encoded pulse sequences and are robust to rf-inhomogeneity.

Fig. 4 shows the experimental results comparing transfer efficiency as a function of rf-mismatch of the three experiments DCP, MOIST and PATCHED experiment.

3 Homonuclear Spins

The methods presented in the previous section, generalize in a straightforward way to homonuclear spins. To fix ideas, we begin by considering two homonuclear spins I and S under magic angle spinning condition. A classical technique for recoupling the spins is the HORROR experiment [13]. The spins are irradiated with an rf-field strength of $\frac{\omega_r}{2}$, where ω_r is the rotor frequency. In a rotating frame, rotating with both the spins at their Larmor frequency, the Hamiltonian of the spin system takes the form

$$H(t)=\omega_I(t)I_z+\omega_S(t)S_z+\omega_{IS}(t)(3I_z S_z - I\cdot S)+\frac{\omega_r}{2}F_x, \quad (10)$$

where the operator $F_x = I_x + S_x$, and $\omega_I(t)$ and $\omega_S(t)$ represent the chemical shift for the spins I and S respectively and $\omega_{IS}(t)$ represents the time varying couplings between the spins under magic-angle spinning. The chemical shifts and the time varying couplings can be expressed using Fourier series as in Eq. (2).

The term $I\cdot S$ in Eq. (10), commutes with the rf-Hamiltonian, $\frac{\omega_r}{2}F_x$, as it averages under MAS. We will, therefore, drop this term in the subsequent treatment. In the interaction frame of the rf irradiation, the internal Hamiltonian from Eq.(1), takes the form

$$H_I(t)=\frac{3}{2}\omega_{IS}(t)Z^- +\frac{3}{2}\omega_{IS}(t)(Z^+\cos(\omega_r t)+Y^+\sin(\omega_r t)), \tag{11}$$

where, X^-, Y^-, Z^- are zero quantum operators and X^+, Y^+, Z^+ are multiple quantum operators as defined before. To begin, we assume that $\omega_I(t)$ and $\omega_S(t)$ are significantly smaller than the rf-power $\frac{\omega_r}{2}$ and therefore, they average out in the interaction frame of the rf-irradiation. The modulation $\cos\omega_r t$, caused by the rf-field, generates a secular term with the modulation due to the MAS. This results in the effective γ encoded Hamiltonian,

$$H_{hom}(\gamma)=\kappa_h[\cos(\gamma)(I_zS_z - I_yS_y) - \sin(\gamma)(I_zS_y+I_yS_z)], \tag{12}$$

where the scaling factor

$$\kappa_h=\frac{3}{4\sqrt{2}}b_{IS}\sin(2\beta) \tag{13}$$

depends on the dipole-dipole coupling constant b_{IS}. In the multiple quantum frame spanned by the operators $\{X^+, Y^+, Z^+\}$, the effective Hamiltonian $H_{hom}(\gamma)$ inverts the initial operator $X^+ \rightarrow -X^+$ and transfers the initial state $I_x \rightarrow S_x$.

3.1 Broadband Homonuclear Recoupling

In practice, $\omega_I(t)$ and $\omega_S(t)$ may be comparable or larger than ω_r, and therefore the proposed methodology is narrow-band and gives poor transfer efficiency in the presence of Larmor dispersion. Subsequently, we will address the problem of making these homonuclear sequences broadband. We first show how the concept of phase alternating pulse sequences can be applied to the present context.

The inhomogeneity is modeled by a parameter ε, such that the rf- Hamiltonian of the system takes the form

$$H^{rf}=\frac{\omega_r}{2}(1+\varepsilon)F_x. \tag{14}$$

In the interaction frame of rf-irradiation along x axis, with strength $\frac{\omega_r}{2}$, the Hamiltonian of the system in (10) averages to

$$H_I=H_{hom}(\gamma)+\varepsilon\frac{\omega_r}{2}F_x. \tag{15}$$

The Hamiltonian gives a poor transfer of the the initial operator $X^+ \rightarrow -X^+$, (and therefore also for the transfer of state $I_x \rightarrow S_x$) when $\varepsilon\omega_r \sim \kappa$, where κ is as in Eq. (12). As seen in Fig. 5A, an ε value of.05, will lead to appreciable loss in the transfer efficiency.

Analogous to experiments in Fig. 3A and Fig. 3C, are the homonuclear recoupling experiments shown in Fig. 5A and Fig. 5B. The experiment in Fig. 5B is phase alternating, γ encoded version

of the experiment in 5A. The analysis of these phase alternating homonuclear experiments is very similar to their heteronuclear counterparts. For sake of completion, we present the analysis here.

In Fig. 5B, in the interaction frame of the x-phase rf-irradiation with strength $\frac{\omega_r}{2}$, in the first and third rotor period, we prepare the effective Hamiltonian,

$$H_1=H_3=H_{hom}(\gamma)+\frac{\varepsilon\omega_r}{2}F_x. \tag{16}$$

In the second rotor period, an effective Hamiltonian

$$H_2=H_{hom}(-\gamma)-\frac{\varepsilon\omega_r}{2}F_x, \tag{17}$$

is prepared.

In the fourth recoupling period (following the half rotor period delay), the effective Hamiltonian,

$$H_4=H_{hom}(-\gamma-\pi)-\frac{\varepsilon\omega_r}{2}F_x, \tag{18}$$

is produced. The net Hamiltonian, to leading order, is then

$$\overline{H}=\frac{H_1+H_2+H_3+H_4}{4}=\frac{2\kappa}{5}\{\cos(\gamma)(I_zS_z-I_yS_y)+\sin(\gamma)(I_zS_y+I_yS_z)\}. \tag{19}$$

Observe, to leading order, the inhomogeneity in the field gets canceled by phase alternation. The recoupling Hamiltonian is scaled down by a factor of $\frac{2}{5}$, compared to standard HORROR experiment. Fig. 6A, shows the transfer efficiency vs mixing time curves for the HORROR experiment shown in the Fig. 5A with different level of rf-inhomogeneity. Fig. 6B shows the transfer efficiency vs mixing time curves for the phase alternating HORROR experiment shown in Fig. 5B. Note, both experiments in Fig. 5A and Fig. 5B are narrowband and work in the regime $\omega_r \gg \omega_I(t), \omega_S(t)$.

In practice, $\omega_I(t)$ and $\omega_S(t)$ may be comparable or larger than ω_r and therefore, the proposed methodology gives poor transfer efficiency in the presence of large Larmor dispersions. We now address the problem of making these homonuclear sequences broadband by a suitable modulation of the rf-field as described below. The main ideas presented here are further developments on the recent work [38] on broadband homonuclear recoupling. The homonuclear recoupling experiments presented [38] are sensitive to rf-inhomogeneity. We now show how the concept of phase alternation can be incorporated to make these experiments immune to rf-inhomogeneity.

Consider the rf-irradiation on homonuclear spin pair whose amplitude is chosen as $A(t)=\frac{C}{2\pi}$ and the offset.$\Delta\omega(t) = \omega_r \sin(Ct)$. This offset is implemented as a phase modulation

$$\varphi(t)=\frac{2\omega_r}{C}\sin^2(Ct)=\frac{\omega_r}{C}(1-\cos(Ct)).$$

so that the rf-Hamiltonian, takes the form

$$H^{rf}(t)=CF_x-\omega_r\sin(Ct)F_z, \tag{20}$$

where C is in angular frequency units and we choose $C \gg \omega_I(t), \omega_S(t), \omega_r$. In the interaction frame of the irradiation along x axis, with the strength C, the coupling Hamiltonian of the spin system takes the form

$$H_I^{DD}(t)=\frac{3}{2}\omega_{IS}(t)(I_zS_z+I_yS_y)+\frac{3}{2}\omega_{IS}(t)((I_zS_z-I_yS_y)\cos Ct+(I_zS_y+I_yS_z)\sin Ct), \tag{21}$$

and the rf-Hamiltonian of the spin system transforms to

$$H_I^{rf}(t)=\frac{\omega_r}{2}(-\cos 2Ct\,F_z+2\sin^2 Ct\,F_y), \tag{22}$$

which averages over a period $\tau_c = 2\π/C$ to

$$H_I^{rf}=\frac{\omega_r}{2}F_y. \tag{23}$$

Now, transforming into the interaction frame of the rf Hamiltonian H_I^{rf}, we only retain terms that give secular contribution to the effective Hamiltonian, i.e., terms oscillating with frequency C are dropped and the residual Hamiltonian takes the form

$$H_{II}(t)=\kappa_h\{\cos(\omega_r t)\cos(\omega_r t+\gamma)(I_zS_z-I_xS_x)+\sin(\omega_r t)\cos(\omega_r t+\gamma)(I_zS_x+I_xS_z)\}, \tag{24}$$

which over a rotor period averages to

$$\overline{H}_{II}=\frac{\kappa_h}{2}\{\cos(\gamma)(I_zS_z-I_xS_x)-\sin(\gamma)(I_zS_x+I_xS_z)\}. \tag{25}$$

where κ_h is as in Eq. (12). The Hamiltonian $\bar{H}_{II}$ performs the transfer $I_y \leftrightarrow S_y$.

This cosine modulated pulse sequence is broadband as a large value of C averages out the chemical shift [38]. The main drawback of the high power cosine modulated pulse sequence is its sensitivity to rf-inhomogeneity. To analyze the effect of inhomogeneity, let ε denote the inhomogeneity parameter. Then, rewriting H_{rf} in Eq. (20) gives

$$H^{rf}(t)=C(1+\varepsilon)F_x - \omega_r \sin(Ct)F_z. \tag{26}$$

In the interaction frame of irradiation along *x* axis with strength *C*, the rf-Hamiltonian averages to $\varepsilon CF_x+\frac{\omega_r}{2}F_y$. Now, proceeding to the interaction frame of the rf Hamiltonian $\frac{\omega_r}{2}F_y$, the total Hamiltonian of the spin system averages to

$$H_{eff}=\overline{H}_{II}+\varepsilon CF_x, \tag{27}$$

where $\bar{H}_{II}$ is as in the equation (25). In this interaction frame, the Hamiltonian $\bar{H}_{II}$ performs the dipolar recoupling. However, for large *C*, the factor εCF_x may significantly reduce the HORROR matching condition.

3.2 PAMORE experiment

Here, we present a method to eliminate this effect of the rf-inhomogeneity by simply phase alternating every $\tau_c=\frac{2\pi}{C}$ units of time, by making $\varphi(t+\tau_c=\pi-\varphi(t)$. We call this pulse sequence PAMORE (**P**hase **A**lternating **MO**dulated **RE**coupling). This results in switching the rf-Hamiltonian every τ_c units of time between

$$H_1^{rf}(t)=(1+\varepsilon)CF_x - \omega_r \sin(Ct)F_z;\ H_2^{rf}(t)=-(1+\varepsilon)CF_x+\omega_r \sin(Ct)F_z \tag{28}$$

The top panels in Fig. 7 show the phase modulation of the rf-field over a rotor period for the CMRR and PAMORE pulse sequences respectively.

To analyze the effect of the pulse sequence, whereby the rf Hamiltonian is switched between $H_1^{rf}(t)$ and $H_2^{rf}(t)$, let us first transform into the interaction frame of the Hamiltonian that switches between CF_x and $-CF_x$, every τ_c units of time.

Therefore, in the first τ_c, one obtains an effective rf-Hamiltonian,

$$H_1^{rf}=\varepsilon CF_x+\frac{\omega_r}{2}F_y, \tag{29}$$

followed by the Hamiltonian

$$H_2^{rf}=-\varepsilon CF_x+\frac{\omega_r}{2}F_y. \tag{30}$$

The effective rf-Hamiltonian one prepares is

$$\overline{H}^{rf}=\frac{H_{rf}^1+H_{rf}^2}{2}=\frac{\omega_r}{2}F_y. \tag{31}$$

If C is chosen large enough, the coupling Hamiltonian $H_I^{DD}(t)$, in the interaction frame takes the form, $\frac{3\omega_{IS}(t)}{2}(I_zS_z+I_yS_y)$, where fast oscillating component at frequency C have been neglected, as they average out. Now, proceeding to the interaction frame of the rf Hamiltonian in Eq. (31), the total Hamiltonian of the spin system averages to H_{II} as in the equation (25). To leading order, the effect of inhomogeneity is canceled out.

Fig. 7 shows simulations comparing the homonuclear recoupling transfer efficiency obtained using CMRR and PAMORE pulse sequence for three different values of ε (0,.02,.05).

The PAMORE pulse sequence can be further compensated against dispersion in the angle β by adiabatically changing the amplitude of the sinusoidally varying offset, i.e,

$$\varphi(t)=m(t)\pi+(-1)^{m(t)}\frac{a(t)}{C}(1+\cos Ct),$$

, where $m(t)$ switches between 0 and 1 every t_c period. This modulation of the phase is depicted in Fig. 7II. This modulation then corresponds to switching between Hamiltonians

$$H^{rf}(\pm)=\pm\{(1+\varepsilon)CF_x-a(t)\sin(Ct)F_z\}. \tag{32}$$

where $a(t)$ is a shaped pulse as described below.

We transform into the interaction frame of the Hamiltonian that switches between CF_x and $-CF_x$, every τ_c units of time. Analogous to Eq. (31), the effective Hamiltonian we prepare over two rotor periods is then

$$\overline{\mathcal{H}}^{rf}=\frac{a(t)}{2}F_y. \tag{33}$$

and the effective Hamiltonian is

$$\overline{\mathcal{H}}^{eff}=\frac{3}{2}\omega_{IS}(t)(I_zS_z+I_yS_y)+\frac{a(t)}{2}(1+\varepsilon)F_y. \tag{34}$$

Now, as $a(t)$ is swept adiabatically (or ramped) from $\omega_r-\Delta$ to $\omega_r+\Delta$, the operator X^+ is inverted to $-X^+$, over the broader range of values of β. This is the standard principle of adiabatic following that guides design of ramped or adiabatic pulses.

4 Results

All experiments were performed on a 360 MHz spectrometer (^{1}H Larmor frequency of 360 MHz) equipped with a triple resonance 4 mm probe. The data from uniformly ^{13}C, ^{15}N -labeled samples of glycine (purchased from Cambridge Isotope Laboratories, Andover, MA) was obtained using the full volume of standard 4 mm rotor at ambient temperature using $\frac{\omega_r}{2\pi}=8$ kHz sample spinning. The experiments used 3s recycling delay, 8 scans, ^{1}H to ^{15}N cross-

polarization with rf-field strength of 54 (^{1}H) and 58–68 (^{15}N ramped) kHz, respectively and duration 1.5 ms.

Fig. 4 shows the experimental ^{13}C spectra for DCP, Phase-alt (MOIST) and PATCHED experiments for the $^{15}N \rightarrow {}^{13}C_{\alpha}$, following the ^{1}H to ^{13}C cross polarization. The experiment used CW decoupling on protons of $\frac{\omega_{rf}^{H}}{2\pi} = 100\,\text{kHz}$ during the transfer. The nominal power on $^{13}C_{\alpha}$ and ^{15}N was calibrated to be $\frac{\omega_{rf}^{C}}{2\pi} = 22.2\,\text{kHz}$ and $\frac{\omega_{rf}^{N}}{2\pi} = 30.2\,\text{kHz}$ to optimize the transfer efficiency of the DCP experiment. The bottom panel in Fig. 4 shows the transfer profile for the DCP, MOIST and PATCHED experiments, when the carbon power is varied from its nominal value. The top panel shows sample spectra from the transfer profile in the bottom panel for discrete values of the $\frac{\omega_{rf}^{C}}{2\pi}$ around the nominal value. The nominal power on $^{13}C_{\alpha}$ and ^{15}N during the half rotor period delays was calibrated to be $\frac{\omega_{rf}^{C}}{2\pi} = 22.2\,\text{kHz}$ and $\frac{\omega_{rf}^{N}}{2\pi} = 20.2\,\text{kHz}$ respectively. The powers are chosen large enough to prevent chemical shift evolution and avoid Hartmann Hahn and rotary resonance conditions and thereby prevent dipolar recoupling. The exact values are experimentally optimized.

As expected from theory and simulations, the MOIST experiment is much more robust to rf-inhomogeneity compared to the standard DCP experiment. However, it is not a γ encoded experiment and therefore has a lower transfer efficiency. The PATCHED experiment is both insensitive to rf-inhomogeneity and γ encoded as seen from Fig. 4.

Fig. 8, shows the experimental spectra for CMRR and PAMORE pulse sequences, for the $^{13}C_{\alpha} \rightarrow {}^{13}CO$ transfer following the ^{1}H to ^{15}N CP transfer and ^{15}N to $^{13}C_{\alpha}$ DCP transfer. The CP and DCP steps used the same rf-powers as calibrated in experiment 1 in Fig. 4. CW decoupling on protons of $\frac{\omega_{rf}^{H}}{2\pi} = 100\,\text{kHz}$ was used during the experiment. The nominal power on ^{13}C channel during the CMRR and PAMORE experiment was calibrated to $\frac{\omega_{rf}^{C}}{2\pi} = 48\,\text{kHz}$ with the carrier placed midway between C_{α} and CO resonances that are 12 kHz apart. The rf-power is chosen sufficiently large to prevent ^{13}C chemical shift evolution and make the recoupling broadband. In principle, sufficiently large power on carbon should also decouple protons.

However, we use conventional CW decoupling on protons of $\frac{\omega_{rf}^{H}}{2\pi} = 100\,\text{kHz}$ and therefore moderate rf power is used on ^{13}C channel for effective decoupling. The phase modulation over one rotor period for the CMRR and PAMORE pulse sequence are shown in panels *I* and *II* in Fig. (7). Both experiments used 15 rotor periods for the full transfer and start with initial y magnetization on $^{13}C_{\alpha}$ following $^{15}N \rightarrow {}^{13}C_{\alpha}$ DCP transfer.

It is evident from the simulation results in Fig. 7 and the experimental data in Fig. 8 that the PAMORE experiment is significantly less sensitive to rf-inhomogeneity. Here we have used modest rf-power of 48 kHz on the ^{13}C channel to make the Homonuclear recoupling broadband. This however requires separate Proton decoupling. By simply increasing the power on the carbon channel, we can eliminate the need for Proton decoupling as the same rf-field on carbon can help to decouple protons. This has been suggested as a merit of the CMRR like pulse sequences as it can significantly reduce sample heating [38]. However, the issue of sensitivity to rf-inhomogeneity becomes even more critical as we use more rf-power on the carbon as argued in Eq. (27). Therefore, the use of PAMORE pulse elements becomes even more critical at high ^{13}C powers.

5 Conclusion

In this article, we reported some new developments based on the concept of phase alternating pulse sequences for the design of heteronuclear and homonuclear recoupling experiments that are insensitive to rf-inhomogeneity. The principle was finally applied to the development of improved homonuclear recoupling experiments.

The techniques presented here can be incorporated in more elaborate experiment design that can also compensate for the dispersion in the angle β in Eq. (5) and Eq. (13). In our recent work [20], we showed that the problem of dipolar recoupling in the presence of anisotropies in β and the strength of rf-field to a problem of control of single spin in the presence of rf-inhomogeneity and Larmor dispersion respectively. Using this analogy, we demonstrated how ideas of composite pulse sequences [21,22,23] from liquid-state NMR can be incorporated in dipolar recoupling experiments to make them insensitive to angle β and rf-inhomogeneity. It is now possible to construct a family of dipolar recoupling experiments of increasing length and degree of compensation that ultimately achieve 100% transfer efficiency for all orientations of the dipolar coupling tensor. However, these composite pulse sequences tend to be long, especially in the presence of rf-inhomogeneity which translates into large Larmor dispersion in the single spin picture. Therefore, elaborate designs are needed to compensate for this rf-inhomogeneity. Based on the methods presented in this paper, significantly shorter composite re-coupling pulse sequences can be engineered based on phase alternating re-coupling blocks. This essentially reduces the problem to compensating only for dispersion in angle β, which takes significantly shorter composite dipolar recoupling experiments.

Furthermore, using gradient ascent algorithms as described in [20,26], it is possible to engineer the shape of $a(t)$ in Eq. (34), which optimizes the compensation against β and rf-inhomogeneity. We will address this problem in future work.

Acknowledgments

The research was supported in part by ONR 38A-1077404, AFOSR FA9550-05-1-0443 and NSF 0724057 and in part by the grants from the National Institutes of Biomedical Imaging and Bioengineering (EB003151 and EB002026).

References

1. Opella SJ. Nat Struct Biol 1997;4:845–848. [PubMed: 9377156]
2. Griffin RG. Nat Struct Biol 1998;5:508–512. [PubMed: 9665180]
3. Castellani F, van Rossum B, Diehl A, Schubert M, Rehbein K, Oschkinat H. Nature 2002;420:98–102. [PubMed: 12422222]
4. Petkova AT, Ishii Y, Balbach JJ, Antzutkin ON, Leapman RD, Deglaglio F, Tycko R. Proc Natl Acad Sci 2002;99:16742–16747. [PubMed: 12481027]
5. Jaroniec CP, MacPhee CE, Baja VS, McMahon MT, Dobson CM, Griffin RG. Proc Natl Acad Sci 2004;101:711–716. [PubMed: 14715898]
6. Schaefer J, McKay RA, Stejskal EO. J Magn Reson 1979;34:443–447.
7. Levitt MH, Suter D, Ernst RR. J Chem Phys 1986;84(8)
8. Gregory DM, Mitchell DJ, Stringer JA, Kiihne S, Shiels JC, Callahan J, Mehta MA, Drobny GP. Chem Phys Letters 1995;246:654–663.
9. Detken A, Hardy EH, Ernst M, Meier BH. Chem Phys Letter 2002:356. 298–304.
10. Wu X, Zilm KW. J Magn Reson A 1993;104:154.
11. Gullion T, Schaefer J. J Magn Reson 1989;81:196–200.
12. Raleigh DP, Levitt MH, Griffin RG. Chem Phys Lett 1988;146:71–76.
13. Nielsen NC, Bildsøe H, Jakobsen HJ, Levitt MH. J Chem Phys 1994;101:1805–1812.

14. Lee YK, Kurur ND, Helmle M, Johannessen OG, Nielsen NC, Levitt MH. Chem Phys Lett 1995;242:304–309.
15. Hohwy M, Jakobsen HJ, Eden M, Levitt MH, Nielsen NC. J Chem Phys 1998;108:2686–2694.
16. Levitt, MH. Encyclopedia of NMR. Wiley; Chichester: 2002. p. 165-196.
17. Haerberlen U, Waugh JS. Phys Rev 1968;175:453–467.
18. Howhy M, Nielsen NC. J Chem Phys 1998;109:3780–3791.
19. Untidt T, Nielsen NC. Phys Rev E 2003;65:021108-1–021108-17.
20. Khaneja N, Kehlet C, Glaser SJ, Nielsen NC. J Chem Phys 2006;124:114503. [PubMed: 16555897]
21. Levitt MH, Freeman R. J Magn Reson 1981;43:65–80.
22. Shaka AJ, Freeman R. J Magn Reson 1983;55:487–493.
23. Levitt MH. Prog NMR Spectrosc 1986;18:61–122.
24. Durr, Melinda. Solid State NMR Spectroscopy. 2000
25. Pontryagin, LS.; Boltyanskii, VG.; Gamkrelidze, RV.; Mishchenko, EF. The Mathematical Theory of Optimal Processes. Interscience; New York: 1962.
26. Khaneja N, Reiss T, Kehlet C, Schulte-Herbruggen T, Glaser SJ. J Magn Reson 2005;172:296–305. [PubMed: 15649756]
27. Kehlet CT, Sivertsen AC, Bjerring M, Reiss TO, Khaneja N, Glaser SJ, Nielsen NC. J Am Chem Soc 2004;126:10202–10203. [PubMed: 15315406]
28. Kehlet C, Vosegaard TV, Khaneja N, Glaser SJ, Nielsen NC. Chem Phys Lett 2005;414:204–209.
29. Bak M, Rasmussen JT, Nielsen NC. J Magn Reson 2000;147:296–330. [PubMed: 11097821]
30. Chingas GC, Garroway AN, Bertrand RD, Moniz WB. J Magn Reson 1979;35:283–288.
31. Chingas GC, Garroway AN, Bertrand RD, Moniz WB. J Chem Phys 1981;74:127–156.
32. Glaser SJ, Quant JJ. Advances in Magnetic and Optical Resonance 1996;19:59–252.
33. Bjerring M, Rasmussen JT, Krogshave RS, Nielsen NC. J Chem Phys 2003;119:8916–8926.
34. Bjerring M, Nielsen NC. Chem Phys Lett 2003;382:671–678.
35. Kobzar K, Skinner TE, Khaneja N, Glaser SJ, Luy B. J Magn Reson 2004;170:236–243. [PubMed: 15388086]
36. Baldus M, Geurts DG, Hediger S, Meier BH. J Magn Reson A 1996;118:140–144.
37. Verel R, Baldus M, Nijman M, Vanus JWM, Meier BH. Chem Phys Lett 1997;280:31–39.
38. De Paëpe G, Bayro MJ, Lewandowski J, Griffin RG. J Amer Chem Soc 2006;128:1776–1777. [PubMed: 16464061]

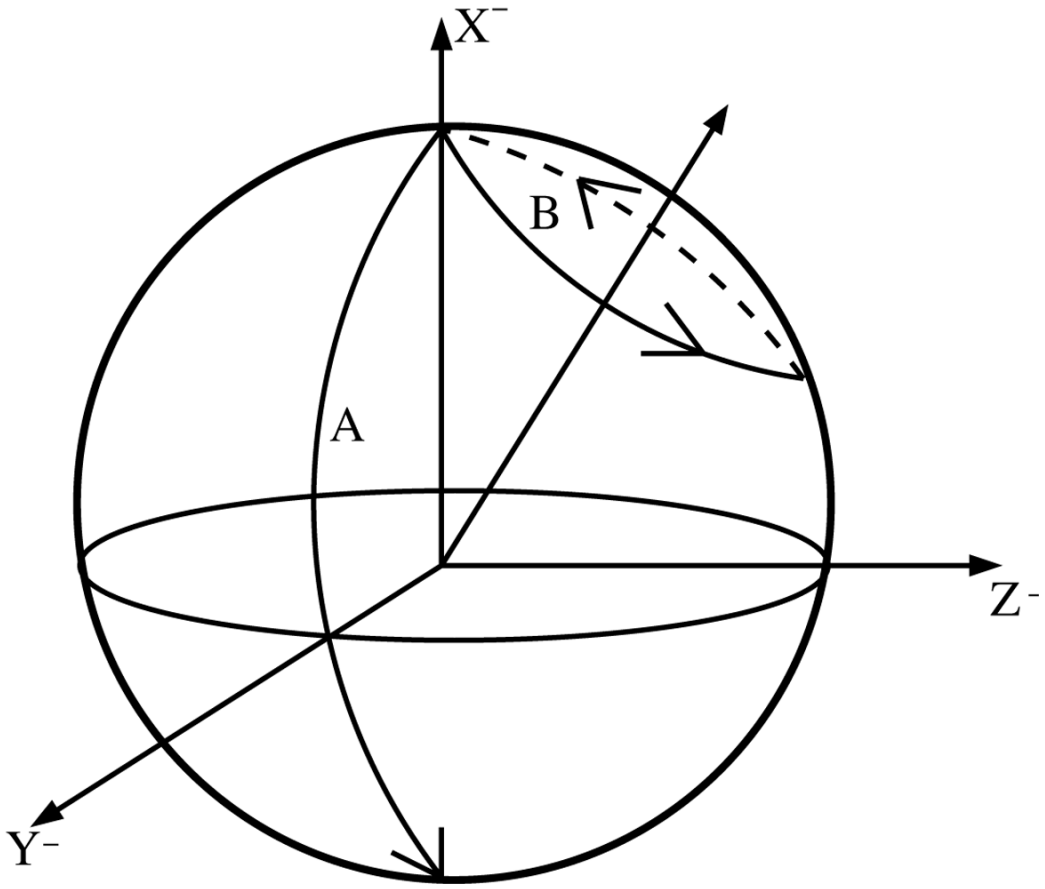

Figure 1.
The figure depicts the zero quantum frame, where the transfer $I_x \rightarrow S_x$ is simply viewed as the inversion of the initial operator $X^- \rightarrow -X^-$. In the presence of rf-inhomogeneity, the inversion is incomplete, as the rotation X^- is performed around the tilted axis as shown in the above figure.

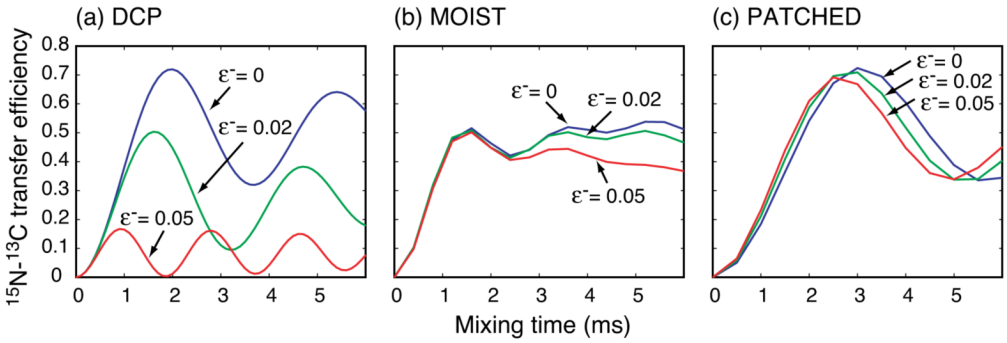

Figure 2.

The above three panels show efficiency η of $^{15}\mathrm{N} \rightarrow {}^{13}\mathrm{C}$, coherence transfer for the DCP, MOIST and PATCHED experiment as a function of the mixing time τ_d, with experimental conditions corresponding to MAS experiments with 10 kHz spinning and using a 360 MHz (Larmor frequency of ^{1}H) magnet. The nominal rf-field strength of $\omega^C_{rf}/2\pi$=50 kHz and $\omega^N_{rf}/2\pi$=40 kHz were used. The calculations used δ^C_{iso}=0, δ^C_{aniso}=19.43 ppm, η^C =.98, $\{\alpha^C_{PR},\beta^C_{PR},\gamma^C_{PR}\}=\{64.9^\circ, 37.3^\circ, -28.8^\circ\}$, δ^N_{iso}=10, δ^N_{aniso}=10.1 ppm, η^N =.17, $\{\alpha^N_{PR},\beta^N_{PR},\gamma^N_{PR}\}=\{-83.8^\circ, -79.0^\circ, 0.0^\circ\}$, and internuclear, distance r_{CN} = 1.52 A°, $\{\alpha^{CN}_{PR},\beta^{CN}_{PR},\gamma^{CN}_{PR}\}=\{0^\circ, 0^\circ, 0^\circ\}$, and J_{CN} = −11 Hz. The rf-power of $\omega^N_{rf}/2\pi$=40kHz, on the nitrogen channel is now changed from the nominal value to $40(1+\bar{\varepsilon})$ Khz. The build up curve for different values of epsilon (expressed in %) are plotted. The top left panel is the standard DCP experiment. The top right experiment is the phase alternating DCP experiment as shown in Fig. 3B, which is not γ encoded. The bottom panel shows the phase alternating DCP experiment which is γ encoded as shown in Fig. 3C. Rf-power of $\omega^C_{rf}/2\pi=\omega^C_{rf}/2\pi$=60 Khz is used on both the channels during the half rotor period delays of $\frac{\tau_r}{2}$ to eliminate chemical shift evolution.

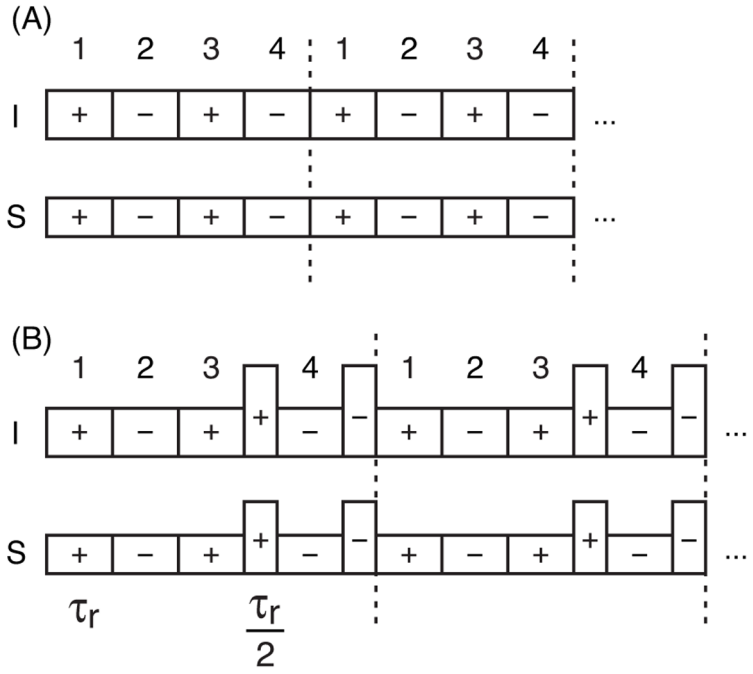

Figure 3.
In Fig. A is shown the basic idea of the MOIST experiment, where the phase of the rf-field is switched every τ_r units of time. In Fig. B is shown the PATCHED experiment, where introducing delays of $\frac{\tau_r}{2}$, preceding and past every fourth period keeps the γ encoding property of the recoupled Hamiltonian. The rf power on both channels during half rotor period delays is chosen to avoid Hartmann Hahn matching and rotary resonance and prevent dipolar recoupling.

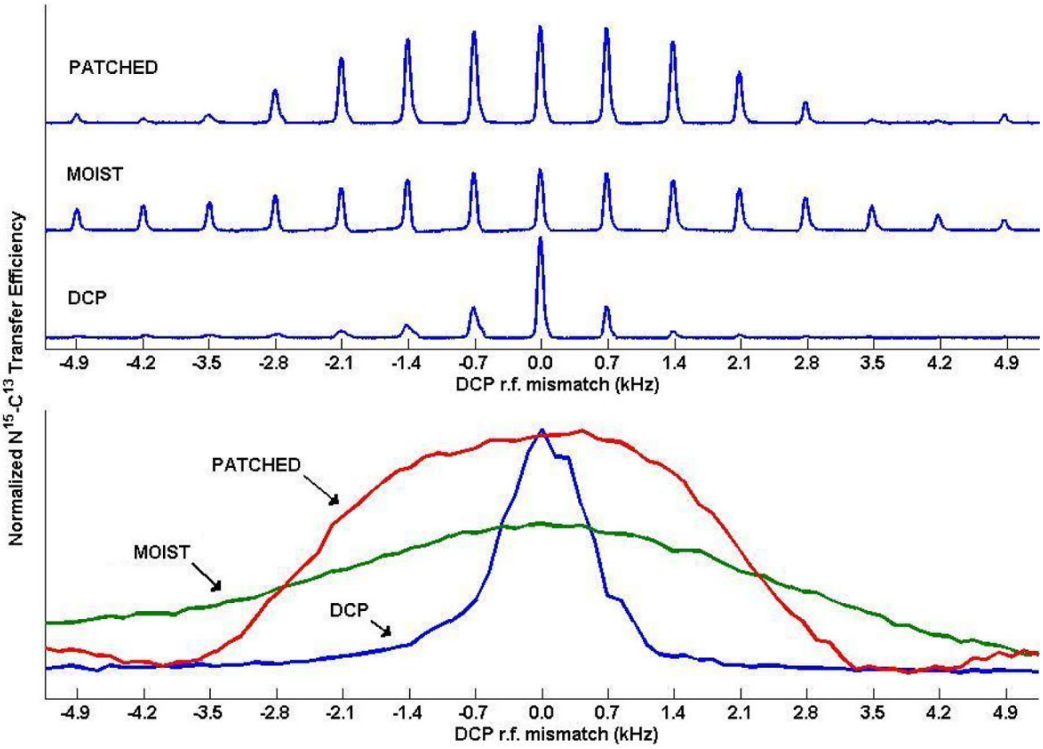

Figure 4.

The above figure shows the experimental spectra for DCP, Phase-alt (MOIST) and PATCHED experiments for $^{15}N \rightarrow ^{13}C_{\alpha}$, transfer for a powder $^{13}C_{\alpha}$, ^{15}N labeled glycine using MAS spinning at $\frac{\omega_r}{2\pi}=8$ Khz and CW decoupling on protons of $\frac{\omega^H_{rf}}{2\pi}=100$ Khz. The nominal power on $^{13}C_{\alpha}$ and ^{15}N was calibrated to be $\frac{\omega^C_{rf}}{2\pi}=22.2$ Khz and $\frac{\omega^N_{rf}}{2\pi}=30.2$ Khz. The bottom panel shows the transfer profile when the carbon power is varied from its nominal value. The top panel shows sample spectra from the transfer profile in the bottom panel for discrete values of the $\frac{\omega^C_{rf}}{2\pi}$ around the nominal value. The nominal power on $^{13}C_{\alpha}$ and ^{15}N during the half rotor period delays was calibrated to be $\frac{\omega^C_{rf}}{2\pi}=22.2$ Khz and $\frac{\omega^N_{rf}}{2\pi}=20.2$ Khz.

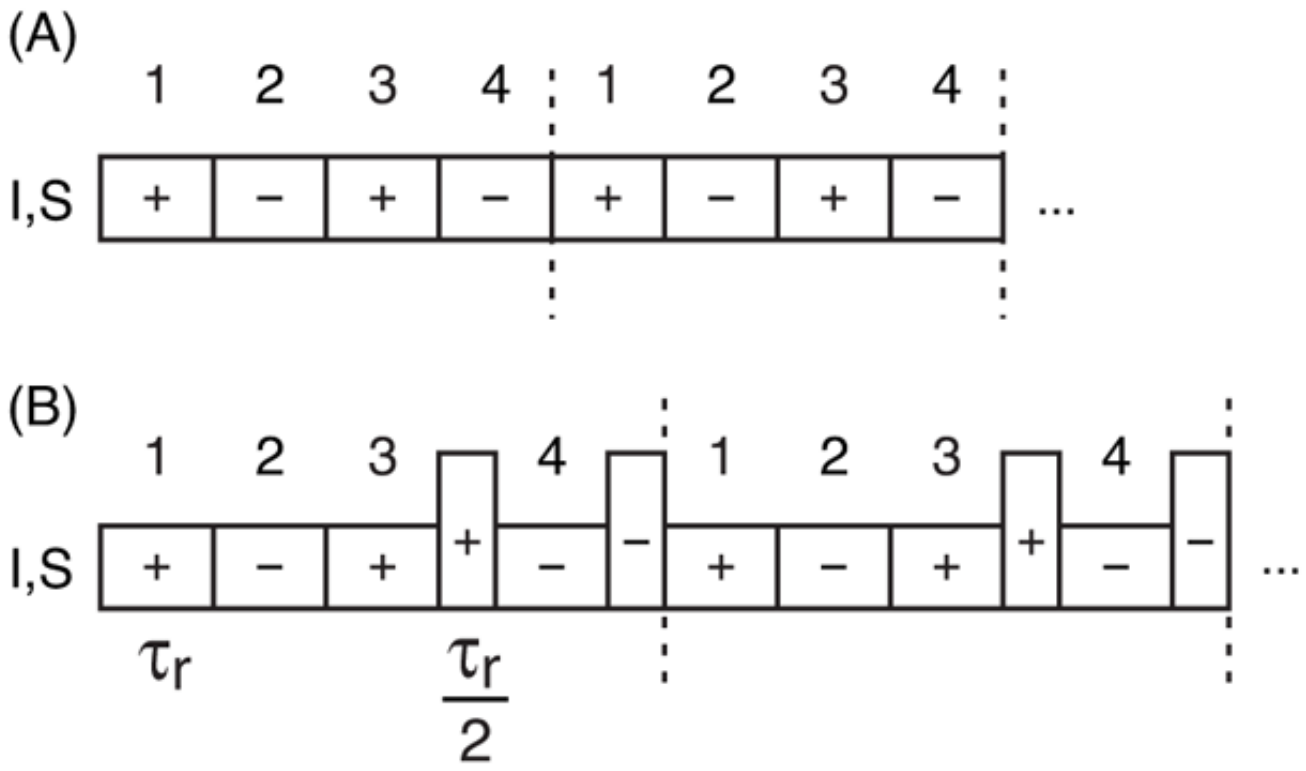

Figure 5.

In Fig. A is shown the phase alternating HORROR experiment, where the phase of the rf-field is switched every τ_r units of time. In Fig. B is shown a modified version of the sequence in Fig. A, where introducing delays of $\frac{\tau_r}{2}$, preceding and past every fourth period keeps the γ encoding property of the recoupled Hamiltonian.

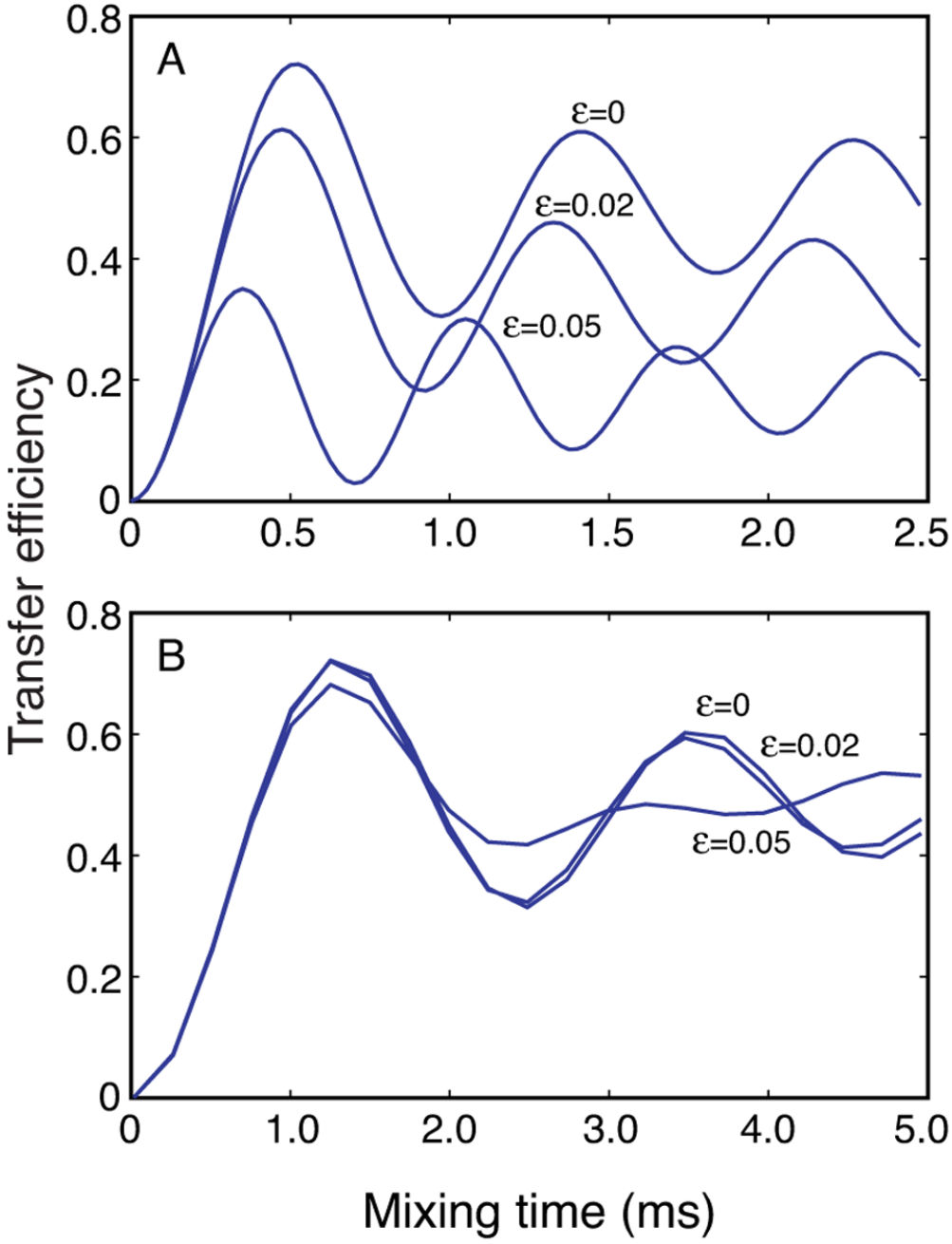

Figure 6.

In Fig. A is shown the transfer efficiency vs mixing time curves for the HORROR experiment (Fig. 5A) with different level of rf-inhomogeneity. Numerical simulation are performed for an on resonance, ^{13}C -^{13}C spin-pair, 1.52 *Å* apart in a powder sample subject to 20 kHz MAS, an external magnetic field corresponding to a 360 MHz (larmor frequency for ^{1}H) spectrometer, and nominal rf-field strength on the ^{13}C channel of 10 kHz. In Fig. B is shown the transfer efficiency vs mixing time curves for the phase alternating HORROR experiment Fig. 5B. Rf-power of $\omega_{rf}^{C}/2\pi$=40 Khz is used during the half rotor period delays of $\frac{\tau_r}{2}$ to prevent chemical shift evolution and recoupling.

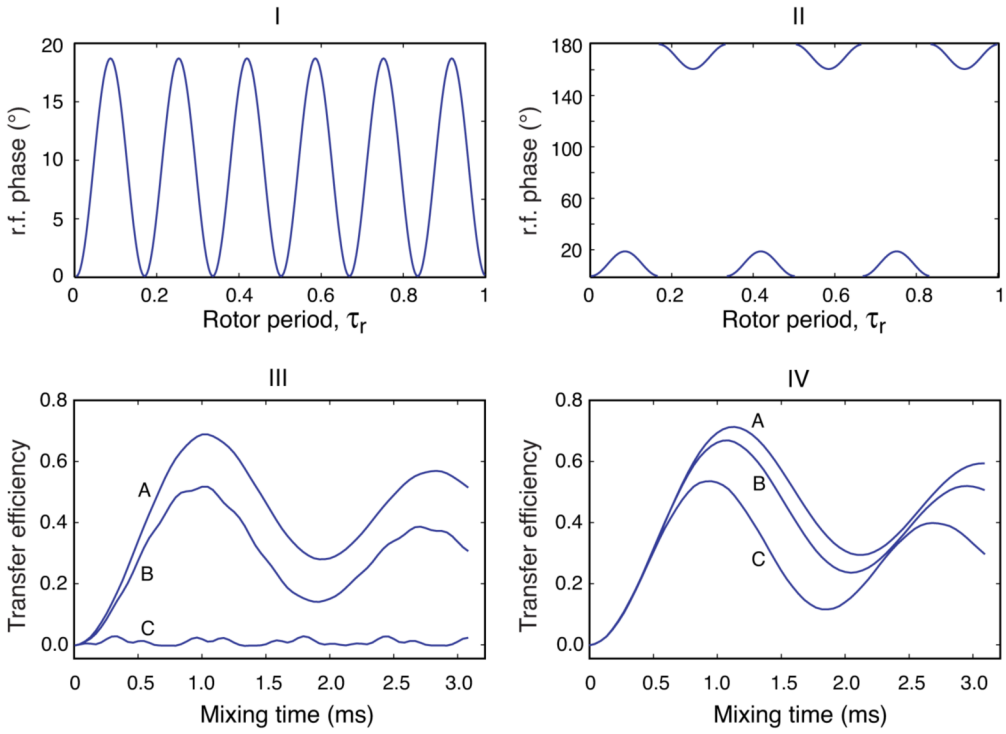

Figure 7.

The top two panels show the phase of the rf irradiation as a function of time (in the units of τ_r) for the CMRR (I) and PAMORE (II) pulse sequences when $C = 8\,\omega_r$. The bottom two panel show numerical simulations of the transfer efficiency for the ^{13}C -^{13}C spin-pair, 1.52 *Å* apart in a powder sample subject to 8 kHz MAS, an external magnetic field corresponding to a 360 MHz (Larmor frequency for ^{1}H) spectrometer and nominal rf-field strength on the ^{13}C channel of 48 kHz, for the CMRR (III) and PAMORE (IV) pulse sequences, for three different values of ε (0,.02,.05) shown as curves *A*, *B* and *C*. Simulations use $C = 6\,\omega_r$, giving $\tau_c = 125/6\,\mu s$ and rf-power of $\omega_{rf}^{C}/2\pi$=48 Khz. The efficiency falls down with increasing ε. In panel *III* at ε =.05, there is almost no transfer.

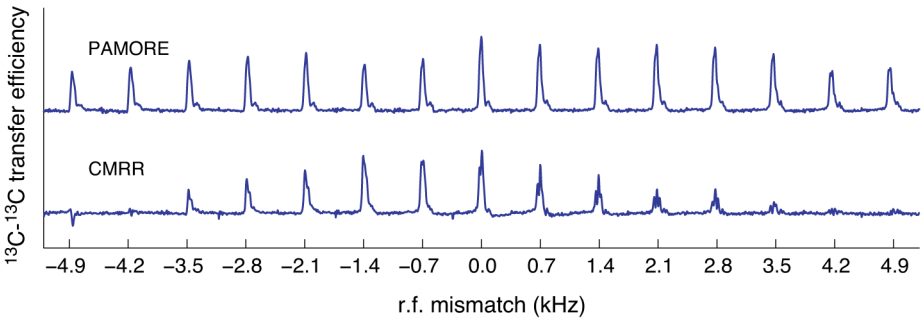

Figure 8.

The top panel shows the experimental spectra for CMRR and PAMORE pulse sequences, $^{13}C_{\alpha} \rightarrow {}^{13b}CO$, transfers for a powder ^{13}C, ^{15}N labeled glycine using MAS spinning at $\frac{\omega_r}{2\pi}=8$ Khz and CW decoupling on protons of $\frac{\omega^H_{rf}}{2\pi}=100$ Khz. The nominal power on ^{13}C channel was calibrated to $\frac{\omega^C_{rf}}{2\pi}=48$ Khz with the carrier placed midway between C_{α} and CO resonances that are 12 KHz apart. The phase modulation over one rotor period for the CMRR and PAMORE pulse sequence are shown in panels *I* and *II* in Fig. (7). Both experiments used 15 rotor periods for the full transfer and start with initial *y* magnetization on $^{13}C_{\alpha}$ following $^{15}N \rightarrow {}^{13}C_{\alpha}$ DCP transfer.